Chinese Chemical Letters 37 (2026) 111560

Contents lists available at ScienceDirect

Chinese Chemical Letters

journal homepage: www.elsevier.com/locate/cclet

"Soft" to "hard" transition and balanced performance in $Pb(Ni_{1/3}Nb_{2/3})O_3$-$Pb(Mn_{1/3}Nb_{2/3})O_3$-$PbZrO_3$-$PbTiO_3$:Sm

Haoran Yu[a], Liang Cao[a], Jiajia Wang[b], Jian Guo[a], Ji Zhang[b], Shan-Tao Zhang[a,*]

[a] National Laboratory of Solid State Microstructures, College of Engineering and Applied Sciences, Nanjing University, Nanjing 210023, China
[b] School of Materials Science and Engineering, Nanjing University of Science and Technology, Nanjing 210094, China

ARTICLE INFO

Article history:
Received 22 April 2025
Revised 30 June 2025
Accepted 8 July 2025
Available online 8 July 2025

Keywords:
$Pb(Ni_{1/3}Nb_{2/3})O_3$-$Pb(Mn_{1/3}Nb_{2/3})O_3$-$PbZrO_3$-$PbTiO_3$
Ceramics
Piezoelectric property
"Soft" and "hard" performance
Domain structure

ABSTRACT

Piezoelectric materials have wide commercial applications involving our everyday lives. The common categorized "soft" and "hard" piezoelectric materials have distinct even contradictory performance parameters typically exemplified by piezoelectric coefficient d_{33} and mechanical quality factor Q_m. However, for some special devices operated in resonant mode, simultaneously high or at least balanced performance parameters are needed. Here, we show the transition from "soft" to "hard" performance in 2 mol% Sm doped $(0.36\text{-}x)Pb(Ni_{1/3}Nb_{2/3})O_3$-$xPb(Mn_{1/3}Nb_{2/3})O_3$–$0.28PbZrO_3$–$0.36PbTiO_3$ quaternary solid solution piezoceramics, for which the d_{33} and planar electromechanical coupling factor k_p decrease, while Q_m and Curie temperature T_c increase monotonously with increasing x value. As the results, balanced performance with moderate $d_{33} = 446$ pC/N, $k_p = 0.49$, $Q_m = 425$, and $T_c = 170$ °C are achieved around $x = 0.03$. This work not only shows the feasibility for combining "soft" and "hard" performance by forming appropriate solid solutions, but also provides a suitable material basis for further simultaneously optimizing piezoelectric parameters.

© 2026 Published by Elsevier B.V. on behalf of Chinese Chemical Society and Institute of Materia Medica, Chinese Academy of Medical Sciences.

Piezoelectric materials with inherent electrical-mechanical conversion capability have been investigated for nearly a century and now not only are commercially utilized in various electronic devices like actuators, sensors, and transducers, but also have potential applications in state-of-art ultra-high power dielectric capacitors, piezoelectric catalysis, and energy harvesters, *etc.* Therefore, piezoelectric materials are one of the research hotspots attracting tremendous long-term scientific activities [1–4]. Among them, inorganic ABO_3 perovskite-structured piezoelectric materials have some unique advantages like thermal stability, high piezoelectric performance, compared to organic or inorganic non-perovskite counterparts. According to the piezoelectric performance, perovskite piezoelectric materials can be classified into "soft" and "hard" categories. In general, "soft" piezoelectric materials by appropriate content donor doping (like rare earth elements doping) exhibit high piezoelectric coefficient d_{33} but low mechanical quality factor Q_m, while the "hard" ones possess relatively low d_{33} but high Q_m. Especially, it is a challenge to achieve high d_{33} and high Q_m simultaneously because these performance parameters are almost inversely proportional, a possible mechanism for this contrast is that the ferroelectric domain wall motion is facilitated, usually arising from donor doping, in "soft" piezoelectric materials whereas the ferroelectric domain wall motion is impeded, usually caused by acceptor doping, in "hard" ones [4–10]. It can be seen that such contradictory scientific origins of "soft" and "hard" performances make it difficult to develop piezoelectric materials with synergistically high d_{33} and high Q_m.

However, for some high-power applications operated in resonant mode exemplified by ultrasonic surgery and underwater imaging, the piezoelectric materials are expected to have high d_{33} and high Q_m simultaneously, because in general, a high d_{33} signifies high sensitivity while a high Q_m indicates low energy loss [9,10]. Accordingly, much efforts have been devoted to develop piezoelectric materials with simultaneously high d_{33} and high Q_m, aiming at combining the "soft" and "hard" performances. The general methods for this aim include designing composite piezoelectric materials or introducing artificial point defect by acceptor or donor doping to balance the performances based on a "soft" or "hard" piezoelectric material. Actually, great achievements have been made based on these methods [9–18]. Meanwhile, it is noted that these methods involve subtle controlling the composition, the distribution and size of second phases, as well as the level of point defect. So, developing a simple but feasible method that can balance "soft" and "hard" performances of piezoelectric materials is interesting and is a supplementation to the above methods.

* Corresponding author.
E-mail address: stzhang@nju.edu.cn (S.-T. Zhang).

https://doi.org/10.1016/j.cclet.2025.111560
1001-8417/© 2026 Published by Elsevier B.V. on behalf of Chinese Chemical Society and Institute of Materia Medica, Chinese Academy of Medical Sciences.

Forming solid solution between two or more different end members is a well-established simple, feasible and most effective way to optimize piezoelectric property. Based on this method, peak piezoelectric property can be achieved when the solid solution locates around the so-called morphotropic phase boundary (MPB) which contains coexisted ferroelectric phases [1,19,20]. It is noted that $Pb(Ni_{1/3}Nb_{2/3})O_3$-$PbZrO_3$-$PbTiO_3$ (PNN-PZ-PT) ternary solid solutions show "soft" piezoelectric performance around MPB region, but the d_{33} increases while Q_m decreases with increasing PNN content, thus "soft" performance with high d_{33} but relatively moderate Q_m can be achieved when PNN content is close to 36 mol% [21,22], while rare earth La or Sm donor doping can further increase its d_{33}, especially, the reported optimizing doping content is around 2 mol% [5,6,23]. On the other hand, $Pb(Mn_{1/3}Nb_{2/3})O_3$-$PbZrO_3$-$PbTiO_3$ (PMnN-PZ-PT) solid solution is reported to show "hard" piezoelectric performance with high Q_m even without acceptor doping [24,25], but relatively low d_{33} even with donor doping and texturing [26]. It is worthy to emphasize that the such "hard" performance of PMnN-PZ-PT solid solution is unique because no acceptor doping is needed, completely different from conventional "hard" piezoelectric materials which is usually related with acceptor doping. Therefore, it is possible to combine "soft" performance of acceptor doped PNN-PZ-PT and "hard" performance of un-doped PMnN-PZ-PT to construct PNN-PMnN-PZ-PT quaternary solid solution system, which may preserve the advantages of each end member, thus, achieve balanced d_{33} and Q_m.

It should be noted that PNN-PT and PMnN-PT binary solid solution systems have the shortcomings of relatively lower ferroelectric Curie temperature T_c at the morphotropic phase boundary (MPB), *i.e.*, $T_c \sim 80$ °C and $T_c \sim 120$ °C for 0.65PNN-0.35PT and 0.65PMnN-0.35PT, respectively [27,28]. On the other hand, the PNN-PZ-PT and PMnN-PZ-PT ternary solid solution systems can have relatively high T_c because of its flexible composition engineering.Moreover, both the ternary systems have higher piezoelectric coefficient and electromechanical coupling factors than the binary systems [4,21,22,24]. Therefore, the ternary systems of PNN-PZ-PT and PMnN-PZ-PT are chosen as the end members to construct quaternary system of PNN-PMnN-PZ-PT.

Based on the above description and by further noting that piezoceramics have some unique merits of flexibility for composition adjusting, by comparing to single crystal and thin film forms, here we start from 2 mol% Sm-doped PNN-PZ-PT ternary solid solution with "soft" piezoelectric performance, progressively introduce PMnN to construct (0.36-*x*)PNN-*x*PMnN-0.28PZ-0.36PT quaternary solid solutions. By synthesizing and investigating the structures, domain, and electrical properties of these piezoceramics systematically, we found that upon increasing *x*, a significant transition from "soft" to "hard" performance occurs, featured by the monotonously decreased d_{33} but increased Q_m. Thus, moderate but balanced piezoelectric parameters of $d_{33} = 446$ pC/N and $Q_m = 425$ are achieved around $x = 0.03$.

The (0.36-*x*)PNN-*x*PMnN-0.28PZ-0.36PT:0.02Sm ($x = 0$–0.06) solid solution piezoceramics were synthesized by a two-step solid-state reaction method. In order to avoid pyrochlore phase, columbite precursors of $NiNb_2O_6$ and $MnNb_2O_6$ were synthesized by weighing the dried NiO/$MnCO_3$ and Nb_2O_5 powders (Sinopharm Chemical Reagent Co., ≥ 98 %) stoichiometrically, ball milling each mixture in ethanol for 24 h, sintering the dried mixture at 1100 °C for 4 h. Both columbite precursors are single phase, as confirmed by X-ray diffraction (XRD) patterns shown in Fig. S1 (Supporting information). Then, the obtained $NiNb_2O_6$, $MnNb_2O_6$, the dried PbO (Aladdin, ≥ 99.9 %), ZrO_2 (Aladdin, ≥ 99.99 %), TiO_2 (Sinopharm Chemical Reagent Co., ≥ 99 %), and Sm_2O_3 (Aladdin, ≥ 99.0 %) powders were weighed stoichiometrically according to the chemical formula of (0.36-*x*)PNN-*x*PMnN-0.28PZ-0.36PT:0.02Sm. The weighed powders were ball milled in ethanol for 24 h, dried at 80 °C, calcined at 850 °C for 2 h, ball milled again for 24 h. At last, the powders mixed with 10 wt% polyvinyl alcohol (PVA) were pressed into green disks with 10 mm in diameter and ~1 mm in thickness, sintered in covered alumina crucibles at 1200 °C for 2 h. To compensate the volatilization of Pb at high temperature, the disks were embedded in the corresponding powders during sintering.

The crystal structures were characterized using XRD (Bruker D8 Advance) on grounded ceramics. The microstructure morphologies were recorded using scanning electron microscopy (SEM, Gemini 500) on polished and thermal etched (1000 °C, 30 min) ceramics. The grain size distribution and average grain size were estimated by using Nano Measurer software by counting more than 100 grains. For electrical tests, the circular surfaces of polished disks with the diameter of ~8.5 mm and the thickness of ~0.5 mm were covered with a thin layer of silver paste and fired at 550 °C for 30 min. The local domain structures were investigated by piezoresponse force microscopy (PFM, MFP-3D) at a scanning frequency of 1 Hz in the Vector PFM mode. The temperature-dependent dielectric constant (ε_r-T) and dielectric loss (tanδ-T) were measured by using an LCR meter (Agilent E4980A) on unpoled samples. The polarization-electric field (P-E) loops were recorded at 1 Hz using a TF2000 analyzer (AixACCT) in silicon oil. The d_{33} was measured on poled ceramics by a Berlincourt-d_{33}-meter (ZJ-6A), the poling was carried out with 30 kV/cm for 20 min at room temperature (~25 °C) in silicon oil. The resonant frequency f_r, anti-resonant frequency f_a, the minimum impedance Z_{min} at resonant frequency and the capacitance C at 1 kHz were measured by the impedance analyzer (Agilent 4284) on poled ceramics. The planar electromechanical coupling factor k_p and Q_m were calculated according to the following formulae:

$$\frac{1}{k_p^2} = \frac{0.398 f_r}{f_a - f_r} + 0.579 \tag{1}$$

$$Q_m = \frac{1}{2\pi f_r Z_{min} C \frac{f_a^2 - f_r^2}{f_a^2}} \tag{2}$$

Fig. 1a plots the XRD patterns of the sintered and grounded (0.36-*x*)PNN-*x*PMnN-0.28PZ-0.36PT:0.02Sm powders. All diffraction peaks are sharp and can be indexed based on perovskite structure, indicating the piezoceramics are well-crystallized without any detectable second phases. The split peaks exemplified by (002)/(200) locating near $2\theta \sim 45°$ where (200) peak is weak, as shown in Fig. 1b, indicate the phase structure of these piezoceramics is close to the rhombohedral-tetragonal MPB region [21,22]. Interestingly, it is obvious that with increasing *x* value, the (200) peak further

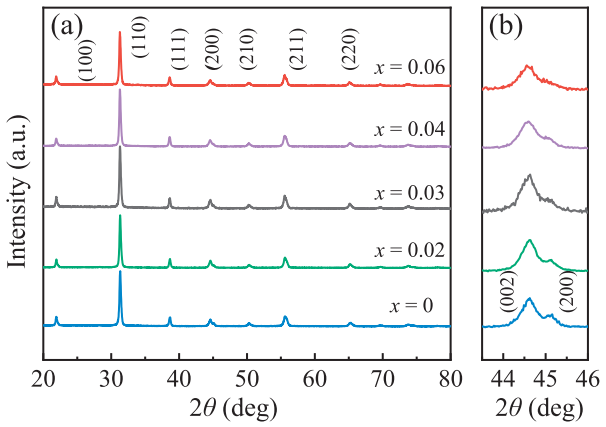


Fig. 1. (a) The XRD patterns and (b) the local enlarged XRD patterns of the (0.36-*x*)PNN-*x*PMnN-0.28PZ-0.36PT:0.02Sm.

weakens progressively and tend to disappear when x reaches 0.06, which implies that the introduction of PMnN leads to slight phase structure evolution away from the MPB toward rhombohedral side. This is reasonable since the different ionic radius of Mn^{2+} (0.83 Å, CN = 6) and Ni^{2+} (0.69 Å, CN = 6) can cause local structure distortion, resulting in octahedron tilting thus changing the macroscopic ratio of rhombohedral and tetragonal phases [29]. Of course, such local structure distortion leads to changed ferroelectric domain morphology and macroscopic properties, as will be shown and discussed in the follows. In addition, it is necessary to emphasize that due to the low PMnN content ($x \leq 0.06$), the lattice constants of these piezoceramics are almost composition-independent, as implied by the fact that the diffraction peaks show negligible shift with increasing x value.

The microstructural morphologies recorded on polished and thermal etched piezoceramics by SEM were comparatively displayed as Figs. S2a-e (Supporting information). One can see that each ceramic has dense microstructure without cracks or voids since the grains are tightly connected. The grain morphology with a polyhedral shape is composition-independent, however, the average grain size decreases monotonously from 2.80 μm for $x = 0$ to 2.36 μm for $x = 0.06$, as plotted in Fig. S2f (Supporting information), the corresponding grain size distribution of each composition is shown in the inset. Since grain size has effect on electrical properties [10,16], such composition dependent grain size will influence the macroscopic properties, as will be discussed below.

In order to better confirm the impact of introducing PMnN component on the (0.36-x)PNN-xPMnN-0.28PZ-0.36PT:0.02Sm system, the typical PFM height, in-plane amplitude, and in-plane phase images within an area of 10×10 μm^2 of the $x = 0$, 0.02, and 0.03 piezoceramics were investigated and illustrated in Fig. 2. It is evident that with the increase of x value, the density of domain wall slightly decreases and the domain size slightly expands with the introduction of PMnN component (Figs. 2d-f). While small-sized domains with low energy barrier means the flattening of Gibbs free energy profile and high domain density, piezoceramics with small-sized domains usually have enhanced piezoelectric properties. What's more, large-sized domains typically are difficult to orient or revert toward the external electric field, which, together with the observed phase structure evolution slightly away from MPB (Fig. 1), contributes to that the $x = 0$ sample exhibits

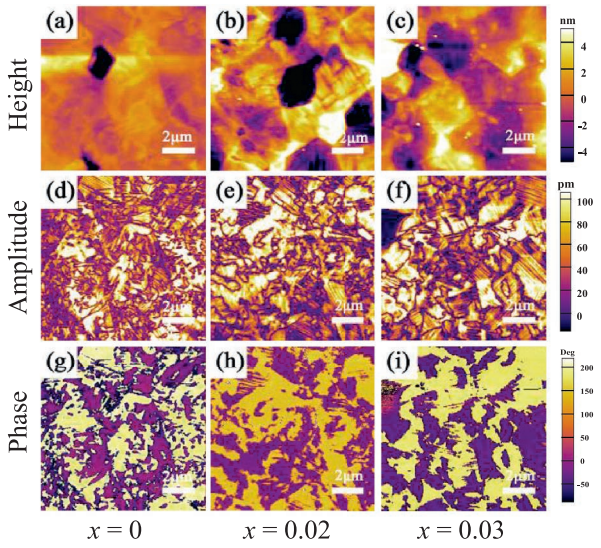


Fig. 2. The PFM height, in-plane amplitude, and in-plane phase images of the (0.36-x)PNN-xPMnN-0.28PZ-0.36PT:0.02Sm piezoceramics. (a, d, g) $x = 0$, (b, e, h) $x = 0.02$, (c, f, i) $x = 0.03$.

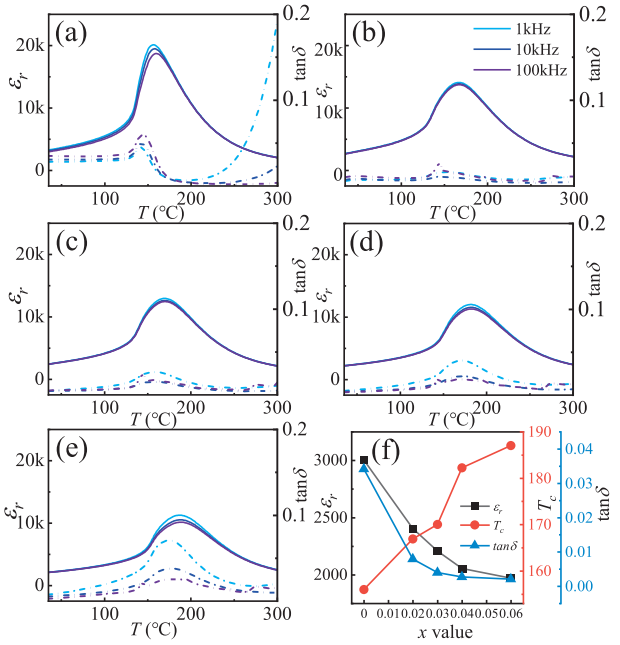


Fig. 3. (a-e) The temperature dependence of ε_r and tanδ of the (0.36-x)PNN-xPMnN-0.28PZ-0.36PT:0.02Sm piezoceramics. (f) composition dependent room temperature ε_r, tanδ, and T_c.

the best piezoelectric properties and with the increase of x value, the piezoelectric properties gradually decrease. Besides, the introduction of PMnN component brings more oxygen vacancies, which assists in pinning the domain wall at the site of defects, thus reduces domain activity and is beneficial to the improvement of Q_m [9]. These results are consistent with the discussion below.

The temperature dependent dielectric constant ε_r and dielectric loss tanδ of the piezoceramics with $x = 0$–0.06 are comparatively illustrated in Figs. 3a-e. Four remarkable features are noticeable. First, the ferroelectric Curie temperature T_c increases with increasing x with the value of 156 °C at $x = 0$ and 187 °C at $x = 0.06$, as shown in Fig. 3f. The PNN-PZ-PT ternary solid solutions have low T_c of $\leq$ 200 °C when PNN content is higher than 10 mol% [21,22], while PMnN-PZ-PT ternary solid solutions have high T_c of $\geq$ 300 °C when PMnN content is lower than 10 mol% [24]. Therefore, it is reasonable that introducing low content PMnN can improve T_c of PNN-PZ-PT. Second, as shown in Fig. 3f, the measured room temperature ε_r decreases upon increasing x, for example $\varepsilon_r = 3002$ for $x = 0$ while $\varepsilon_r = 1971$ for $x = 0.06$ at 1 kHz. Such decreased ε_r can be attributed to two factors. On the one hand, the variable chemical valance of Mn ions or substitution of Mn ions for Zr/Ti ions can induce charged oxygen vacancy, *e.g.*, $MnO \xrightarrow{ZrO_2,TiO_2} Mn''_{Zr,Ti} + O_O^{\times} + V_O^{\cdot\cdot}$, thus exert significant pinning effect of ferroelectric domains to restrict domain switching. Moreover, the local lattice distortion induced by introducing PMnN causes phase structure evolution as discussed above, which actually reduces directional displacement of B-site ions. Both the suppressed domain switching and reduced directional displacement can decrease the contribution of domain wall motion to dielectric constant. On the other hand, the decreased average grain size implies the increased amount of grain boundary, which usually show weak dielectric performance and therefor is conducive to decline macroscopic dielectric constant value. Third, from Fig. 3f one can see that the dielectric loss tanδ also decreases significantly with increasing x and tends to have a low value of ~0.003 when $x \geq 0.03$, which is consistent with the continuously decreased dielectric constant ε_r since both the trapped defects or carriers and

increased amount of grain boundary can inhibit the long-range migration of defects or carries, leading to decreased dielectric loss tanδ. It is worthy to note that these factors for reducing dielectric loss are also conducive for reducing mechanical loss [30,31], which is the reciprocal of Q_m dielectric loss. Thus, it is reasonable to expect that the (0.36-x)PNN-xPMnN-0.28PZ-0.36PT:0.02Sm piezoceramics shall have increased Q_m. Fourth, all the ceramics show slight relaxor behavior as confirmed by the slight frequency dependent peak dielectric constant temperature. It should be noted that the difference between the peak dielectric constant temperatures measured at 1 kHz and 100 kHz, $\Delta T_{1kHz,100\ kHz}$ decreases from 4 °C at $x=0$ to ~0 °C when $x \geq 0.02$, indicating the suppressed relaxor behavior due to the introduction of PMnN.

The room temperature ferroelectric *P-E* loops and *J-E* curves of the (0.36-x)PNN-xPMnN-0.28PZ-0.36PT:0.02Sm piezoceramics are measured at 30 kV/cm (Figs. S3a-e in Supporting information). One can see that each ceramic displays well-saturated *P-E* loop, indicating the ferroelectric nature, which is further reaffirmed by the double-peak *J-E* curve since the peak current arises from ferroelectric domain switching. To compare the composition dependence of ferroelectricity, the characteristic parameters of maximum polarization P_m, remnant polarization P_r, and coercive field E_c are illustrated in Fig. S3f (Supporting information) as a function of x value. Clearly, P_m and P_r have the same composition dependence, both increase slightly with values of 35.7, 26.5 μC/cm^2 at $x=0$ while 39.4, 29.1 μC/cm^2 at $x=0.02$, respectively. Such slight increase of polarization is attributed to that when low amount of PMnN is introduced into 0.36PNN-0.28PZ-0.36PT, the quaternary solid solution persists the rhombohedral-tetragonal MPB structure but the rhombohedral phase ratio increases slightly as discussed above, while rhombohedral phase has 8 possible polarization directions but tetragonal phase has 6 directions, which means the easy domain rotation and thus enhanced contribution to polarization [32]. Upon further increasing PMnN content, the quaternary solid solution further deviates from the MPB, so the polarization decreases. On the contrary, the E_c have opposite composition dependence to P_m and P_r. The lowest E_c occurs at $x=0.02$ with the value of 7.9 kV/cm, then the E_c increases monotonously to 9.2 kV/cm at $x=0.06$. This observation can be attributed to two factors. One is that the increased rhombohedral phase ratio or decreased tetragonal phase ratio as function of x value, in general tetragonal phase has fewer polarization direction compared to rhombohedral phase, thus higher field is needed to trigger domain switching. And the other is that the decreased grain size with increasing x value, which increases grain boundary and promote domain wall pinning and thus is conducive to increase E_c.

Fig. 4 shows the composition dependent d_{33}, Q_m, and planar electromechanical coupling factor k_p of the (0.36-x)PNN-xPMnN-0.28PZ-0.36PT:0.02Sm piezoceramics. It is noted that the d_{33} value of $x=0$ is comparable with that of polycrystalline counterpart but lower than that of textured counterpart [21,22]. With increasing x, the d_{33} and k_p decreases from $d_{33}=637$ pC/N and $k_p=0.59$ at $x=0$ to $d_{33}=337$ pC/N and $k_p=0.37$ at $x=0.06$, on the contrary, the Q_m increases dramatically from $Q_m=58$ at $x=0$ to $Q_m=895$ at $x=0.06$. Such results are reasonable since with introducing PMnN into Sm doped 0.36PNN-0.28PZ-0.36PT, the initially facilitated domain wall motion by Sm-doping tend to be impeded by Mn-induced oxygen vacancy, *e.g.*, $MnO \xrightarrow{ZrO_2,TiO_2} Mn''_{Zr,Ti} + O_O^{\times} + V_O^{\cdot\cdot}$, and this effect becomes more predominant with increasing PMnN content. As the results, a transition from "soft" to "hard" piezoelectric performance occurs in the (0.36-x)PNN-xPMnN-0.28PZ-0.36PT:0.02Sm system. The balanced piezoelectric performance with moderate $d_{33}=446$ pC/N, $k_p=0.49$, $Q_m=425$ are obtained at $x=0.03$. It is interesting to note that the product of d_{33} and Q_m ($d_{33}\times Q_m$) is an important parameter. In our cases, with increasing x value, the d_{33} decreases while Q_m increases, which leads to monotonously increasing $d_{33}\times Q_m$. However, the composition with balanced "soft" and "hard" piezoelectric performance shows high $d_{33}\times Q_m$ of 189,550 pC/N.

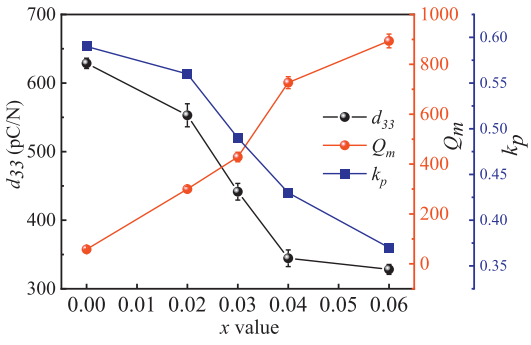


Fig. 4. The composition dependent d_{33}, k_p, and Q_m.

In summary, (0.36-x)PNN-xPMnN-0.28PZ-0.36PT:0.02Sm quaternary solid solution piezoceramics were synthesized and investigated. With increasing x, the phase structure persists close to rhombohedral-tetragonal MPB but the rhombohedral phase ratio increases while the average grain size reduces. More interestingly, the introducing of PMnN triggers a transition from "soft" to "hard" piezoelectric performance, featured by monotonously decreased d_{33} and k_p but increased Q_m and T_c. The balanced piezoelectric performance with moderate $d_{33}=446$ pC/N, $k_p=0.49$, $Q_m=425$, and $T_c=170$ °C are achieved around $x=0.03$. We believe this work is helpful for further work on developing high performance piezoelectric materials with balanced or synergistically improved piezoelectric parameters of d_{33} and Q_m.

CRediT authorship contribution statement

Haoran Yu: Data curation. **Liang Cao:** Data curation. **Jiajia Wang:** Data curation. **Jian Guo:** Formal analysis. **Ji Zhang:** Writing – original draft. **Shan-Tao Zhang:** Writing – review & editing, Writing – original draft, Formal analysis.

Declaration of competing interest

The authors declare that they have no known competing financial interests or personal relationships that could have appeared to influence the work reported in this paper.

Acknowledgments

This work was supported by the National Key R&D Program of China (No. 2020YFA0711504), the National Natural Science Foundation of China (Nos. 12374084 and 12174179), the Dengfeng B Project of Nanjing University.

Supplementary materials

Supplementary material associated with this article can be found, in the online version, at doi:10.1016/j.cclet.2025.111560.

References

[1] G.H. Haertling, J. Am. Ceram. Soc. 82 (1999) 797–818.
[2] S.L. Xie, Y.Y. Chen, Q. He, et al., Chin. Chem. Lett. 35 (2024) 108871.
[3] Y.Q. Zhu, H.H. Chen, L. Wang, et al., Chin. Chem. Lett. 35 (2024) 108884.
[4] L. Chen, H. Liu, H. Qi, et al., Prog. Mater. Sci. 127 (2022) 100944.
[5] L. Bian, X.D. Qi, K. Li, et al., J. Eur. Ceram. Soc. 41 (2021) 6983–6990.
[6] Q. Guo, F. Li, F. Xia, et al., ACS Appl. Mater. Interfaces 11 (2019) 43359–43367.
[7] L. He, D. Vanderbilt, Phys. Rev. B 68 (2003) 134103.

[8] W. Wang, Z. Chen, Z. Zhou, et al., ACS Appl. Mater. Interfaces 15 (2023) 15636–15645.
[9] Z. Li, H.C. Thong, Y.F. Zhang, et al., Adv. Funct. Mater. 31 (2021) 2005012.
[10] G.H. Wang, P.R. Ren, X.C. Qi, et al., J. Eur. Ceram. Soc. 45 (2025) 117363.
[11] Y. Yan, K.H. Cho, S. Priya, J. Am. Ceram. Soc. 94 (2011) 4138–4141.
[12] W. Xiao, Z.R. Chen, X.W. Liu, et al., Mater. Horiz. 11 (2024) 5285–5294.
[13] Y.T. Wu, Y. Cheng, S.Y. Guan, et al., Inorg. Chem. 62 (2023) 15094–15103.
[14] M. Slabki, K.V. Lalitha, J. Rödel, et al., Acta Mater. 227 (2022) 117703.
[15] J.N. Shao, M.P. Zheng, X. Gao, et al., Appl. Phys. Lett. 125 (2024) 082902.
[16] Z.L. Geng, M.P. Zheng, T.C. Ma, et al., ACS Appl. Mater. Interface 17 (2025) 12458–12466.
[17] X.Y. Qiu, C. Wu, D.Q. Tan, et al., Nat. Commun. 16 (2025) 2894.
[18] F.F. Guo, Q. Zhou, Y.F. Chen, et al., J. Am. Ceram. Soc. 106 (2022) 5258–5268.
[19] T.R. Shrout, S.J. Zhang, J. Electroceram. 19 (2007) 111–124.
[20] L.L. Fan, L.X. Zhang, Y. Ren, et al., Inorg. Chem. 59 (2020) 13632–13638.
[21] Q. Wang, L. Bian, S. He, et al., J. Alloy. Compd. 1002 (2024) 175249.
[22] Q. Wang, L. Bian, K. Li, et al., J. Mater. Sci. Technol. 175 (2024) 258–265.
[23] J. Guo, M.Y. Yan, H.R. Yu, et al., Dalton Trans. 53 (2024) 16054–16065.
[24] M. Takahashi, N. Tsubouchi, M. Yonezawa, et al., J. Jpn. Soc. Powder Powder Met. 20 (1974) 274–284.
[25] B.S. Li, G.R. Li, Q.R. Yin, et al., J. Phys. D: Appl. Phys. 38 (2005) 1107–1111.
[26] E.J. Kim, S.W. Kim, D.S. Kim, et al., J. Eur. Ceram. Soc. 43 (2023) 1912–1922.
[27] H.R. Yu, J. Guo, J.J. Wang, et al., Danton Trans. 53 (2024) 11713–11719.
[28] S. Gentil, D. Damjanovic, N. Setter, J. Eur. Ceram. Soc. 25 (2005) 2125–2128.
[29] Z. Tan, S.X. Xie, L.M. Jiang, et al., J. Materiomics 5 (2019) 372–384.
[30] G. Liu, S.J. Zhang, W.H. Jiang, et al., Mater. Sci. Eng. R 89 (2015) 1–48.
[31] Y. Sasaki, S. Takahashi, S. Hirose, Jpn. J. Appl. Phys. 36 (1997) 6058–6061.
[32] B.T. Gao, H. Qi, H. Liu, et al., Chin. Chem. Lett. 35 (2024) 108598.